Available online at www.sciencedirect.com

SCIENCE DIRECT®

J. Chem. Thermodynamics 36 (2004) 211–222

JCT

www.elsevier.com/locate/jct

A novel non-intrusive microcell for sound-speed measurements in liquids. Speed of sound and thermodynamic properties of 2-propanone at pressures up to 160 MPa

R. Gomes de Azevedo [a], J. Szydlowski [a,c], P.F. Pires [a], J.M.S.S. Esperança [b], H.J.R. Guedes [b], L.P.N. Rebelo [a,*]

[a] *Instituto de Tecnologia Química e Biológica, ITQB 2, Universidade Nova de Lisboa, Av.República, Apartado 127, 2780-901 Oeiras, Portugal*
[b] *REQUIMTE, Departamento de Química, Faculdade de Ciências e Tecnologia, Universidade Nova de Lisboa, 2829-516 Caparica, Portugal*
[c] *Department of Chemistry, Warsaw University, Zwirki i Wigury 101, 02-093 Warsaw, Poland*

Received 25 June 2003; accepted 2 December 2003

Abstract

A novel high-pressure, ultrasonic cell of extremely reduced internal dimensions ($\sim 0.8 \cdot 10^{-6}$ m^3) and good precision for the determination of the speed of propagation of sound in liquids was conceived and built. It makes use of a non-intrusive methodology where the ultrasonic transducers are not in direct contact with the liquid sample under investigation. The new cell was used to carry out speed of sound measurements in 2-propanone (acetone) in broad ranges of temperature ($265 < T/\mathrm{K} < 340$) and pressure ($0.1 < p/\mathrm{MPa} < 160$). ($p, \rho, T$) data for acetone were also determined but in a narrower T, p range (298 to 333 K; 0.1 to 60 MPa). In this interval, several thermodynamic properties were thus calculated, such as: isentropic (κ_s) and isothermal (κ_T) compressibility, isobaric thermal expansivity (α_p), isobaric (c_p) and isochoric (c_v) specific heat capacity, and the thermal pressure coefficient (γ_v). Comparisons with values found in the literature generally show good agreement.

Keywords: Speed of sound; Density; Pressure effects; 2-Propanone; Acetone

1. Introduction

Measurements of the speed of sound (SS), u, in liquids have proven to constitute a powerful source of valuable information about the thermophysical properties of chemical substances and their mixtures [1,2]. Most of the SS data reported in the literature have been obtained via so-called intrusive or invasive methods, where both the transmitter and receiver of the acoustic wave are in direct contact with the media under investigation [3–5], while in a few cases non-intrusive methods have been used [5–9]. The non-intrusive SS cell used in the current work is distinct from other non-intrusive ones in two respects: (a) no long buffer rods are used (instead, it presents a unique internal shape) and; (b) the internal volume was decreased by one or two orders of magnitude. Commonly, the volume of the liquid to be used is relatively great (typically, of the order of tens or hundreds of cm^3). The present work reports the development made at the *ITQB* laboratories in Oeiras of an ultrasonic cell and its apparatus for measuring the speed of sound propagation in liquids, which makes use of a non-intrusive method using an extremely reduced liquid volume ($\sim 0.8 \cdot 10^{-6}$ m^3). For this purpose, we designed and built a compact microcell that permits the measurements to be performed by locating the transducers (piezoelectrics) outside the liquid under study. The main advantages of this methodology over traditional invasive and large-volume methods are: (i) the possibility of undertaking measurements on almost any type of liquid, even if it is aggressive or reactive to the piezoelectric materials; (ii) the avoidance

* Corresponding author. Fax: +351-21-4411-277.
E-mail address: luis.rebelo@itqb.unl.pt (L.P.N. Rebelo).

0021-9614/$ - see front matter
doi:10.1016/j.jct.2003.12.001

of possible damage to the piezoelectrics and/or their electric contacts upon pressurization; (iii) the easy generation of high pressures; (iv) the possibility of undertaking studies in metastable regimes, e.g., liquids under tension and/or supercooled; (v) the ability to obtain measurements of SS in very expensive fluids, e.g., isotopically substituted ones. The three latter points are a direct consequence of the extremely reduced volumes involved.

With the dual purpose of testing the novel microcell and associated methodology as well as determining extended high-accuracy data for an important fluid, acetone (2-propanone) was chosen to carry out SS measurements in a broad range of temperature ($265 < T/\mathrm{K} < 340$) and pressure ($0.1 < p/\mathrm{MPa} < 160$). Due to a surprising lack of extensive high quality data for this compound (considering its importance and popular use) even at low pressure, we have also measured at the *REQUIMTE* laboratories in Caparica its SS up to 60 MPa using a high-accuracy standard technique [3] which makes use of a double pulse-eco method. To the best of our knowledge there exists only one report [10] on the pressure dependence of the speed of sound in acetone at three isotherms.

This new microcell will be very useful in systematic investigations of the physical properties of various liquids and their mixtures under extreme (p, T) conditions, especially if speed of sound data can be combined with those of density. To this end, a more detailed analysis of the data from the literature revealed that precise density data for acetone [11–14] are only known for very limited temperature and pressure values (mostly at 298 K and 0.1 MPa) and there is, thus, a need to perform more systematic measurements of density. Therefore, we have also carried out such measurements in the temperature range (298 to 333) K and up to 60 MPa. Kooner and Van Hook [15] investigated the deuterium isotope effect on several thermodynamic properties of acetone (perprotonated (-h) versus perdeuterated (-d)). The combined results of the speed of sound and density allowed us to calculate other physical properties of acetone such as isoentropic (κ_s) and isothermal (κ_T) compressibilities, isobaric thermal expansivities (α_p), isobaric (c_p) and isochoric (c_v) specific heat capacities and thermal pressure coefficients (γ_v). Whenever available, these values are compared with literature data obtained via other methods.

2. Experimental

2.1. Novel acoustic cell

In order to measure the speed of propagation of sound waves in liquids using a non-intrusive method, a new cell was designed and built (figure 1). It consists roughly of a 316 stainless steel hollow, thick-wall cylinder (diameter and length are approx. 30 mm and 36 mm, respectively) where two 1 MHz piezoelectric transducers (PZT), one acting as a transmitter and the other as a receiver, are housed in specially designed compartments in the outer section of the cylinder. They are firmly fixed to this outer segment of the stainless steel walls of the cavities, and, additionally, a thin layer of silicone oil has been placed between the PZTs and the stainless steel to achieve better surface contact (thus, enhancing the transmission of the sound wave). After many attempts, the internal geometry was optimised in order to obtain a clean, low-noise acoustical wave signal, highly sensitive to solvent, temperature, and pressure changes. That optimal geometry comprises (in longitudinal section) an "H-shaped" volumetric form. Generally speaking, this type of internal geometry is of vital importance as it forces the sound waves to travel through the liquid while delaying those travelling through the stainless steel body of the cell. The unwanted signals arising from other directions than those containing the liquid reach the receiver later than the main signal. A patent approval (patent filed) has been requested for the current microcell. The total internal volume of the cell (and, the liquid) is very small (less than $\sim 0.8 \cdot 10^{-6}$ m^3). The transducers are 3 mm diameter, 2 mm thick discs made of a polarised piezoelectric ceramic of lead-titanate-zirconate ($PbZrO_3/PbToO_3$). A thin film of silver was deposited on both of their faces, to serve as an electrode. Both PZTs are separated from the liquid sample by a 2 mm wall of stainless steel. Thus, the main wave leaves the transmitter PZT travelling, first through, ca. 2 mm of stainless steel, then along a ca. 9 mm liquid path, and finally, along 2 mm more of stainless steel, after which it reaches the receptor ultrasonic receptor. Although the fundamental resonance frequency of the ultrasonic transducers is 1 MHz, it was

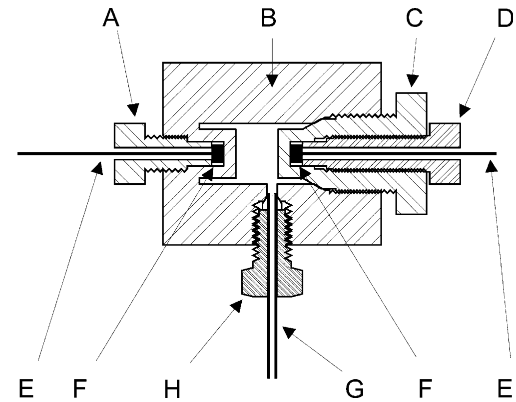

FIGURE 1. Schematic representation of the non-intrusive acoustic microcell with an internal volume of $\sim 0.8 \cdot 10^{-6}$ m^3. A and D, caps holding the PZTs; B, stainless steel cylindrical body; C, cell closure; E, wires for electrical connections; F, piezoelectric transducers; G, 1/16″ tubing; H, high-pressure fitting.

found that the optimal operational frequency is 0.5 MHz. This can be attributed to the fact that the PZT discs are contained in and fixed to a cavity in the body of the cell, which restricts their vibration modes. Electrical connections to the PZTs were made via multi-wired coaxial cables.

The apparatus, schematically shown in figure 2, was built using standard high-pressure valves, 1/16″ thick-walled tubing, and connectors (HIP). It includes a pressure generator (HIP- model 37-6-30) of $11 \cdot 10^{-6}$ m^3 volume equipped with Teflon sealing o-rings, capable of reaching pressures of the order of 200 MPa. Pressure is measured using an Omega pressure transducer, which was calibrated against a high-accuracy Heise gauge. Pressure is measured to both a precision and accuracy better than ±0.05%. In the case of low-cost, low-viscosity, relatively high-vapour pressure fluids (such as acetone) the entire apparatus (pressure generator, pressure sensor, tubing, etc.) is completely filled with the liquid under investigation. Thus, the liquid simultaneously acts as the liquid sample under study and hydraulic fluid as well. Otherwise, the liquid sample only occupies volumes corresponding to the cell and buffer lines. The buffer lines prevent the presence of any traces of hydraulic fluid at any time inside the cell, which would certainly occur upon several pressurization cycles. The acoustic cell is placed in a Hart Scientific calibration bath (stability ±0.001 K) and the temperature is measured by a 4-wire platinum resistance thermometer (PRT) coupled with a Keithley digital multimeter (Model DMM 199). The PRT was previously calibrated, thus allowing temperature measurements on the ITS-90 scale with an estimated uncertainty better than ±0.01 K.

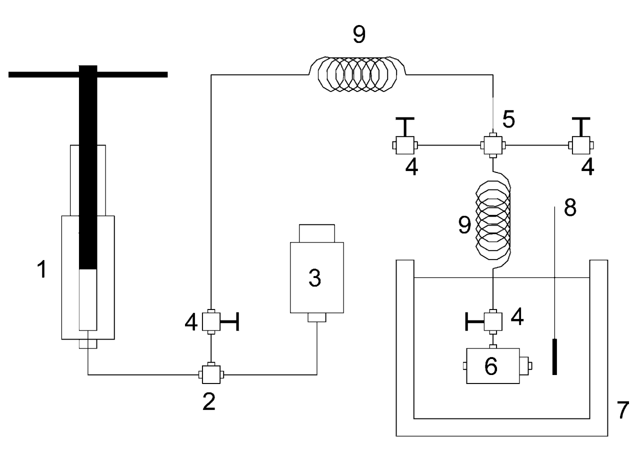

FIGURE 2. Schematic representation of the high-pressure apparatus for the speed of sound measurements: 1, high-pressure generator (screw injector); 2, three-way connector; 3, pressure transducer; 4, high-pressure valves; 5, four-way connector; 6, acoustic microcell; 7, thermostatic bath; 8, platinum resistance thermometer; 9, 1/16″ tubing of buffer line.

2.2. Measurements and chemicals

To measure the speed of sound, a 0.5 MHz, 16 V peak-to-peak sinusoidal wave is fed to the transmitter PZT through a Wavetek 50 MHz function generator (Model 80). The signal passes through the metal, the liquid, and the metal again, and it is recognized by the receiver PZT. The response signal is then amplified and sent to a digital oscilloscope (Tektronix, model TDS 3032) where it is analysed. By measuring the total time period between the two instants (the time delay between the initial and final signals, the so-called Time of Flight, $\Delta\tau$), one can determine the speed of sound in the liquid. Ideally, this total time is the sum of the periods of time that the wave remains in the two 2 mm thickness stainless steel walls followed by the 9 mm long liquid path. Were both these dimensions and the SS in the stainless steel known to very high accuracy (and as a function of p and T), one could easily determine the SS in the liquid, u, by simple difference between these two terms,

$$1/u = K\Delta\tau - KK', \tag{1}$$

where K and K' are functions weakly dependent on T and p and related, respectively, to the acoustic thickness of the liquid and the acoustic thickness and SS in the metal. In practice, this is not feasible, and a calibration procedure has to be followed. The cell was calibrated by measuring the $\Delta\tau$ of toluene, water, ethanol and tetrachloromethane over broad ranges of pressure ($0.1 < p/\text{MPa} < 175$), temperature ($278.15 < T/\text{K} < 338.15$) and SS ($800 < u/\text{m}\cdot\text{s}^{-1} < 2000$) using a total of 120 data points, and fitting the data along with the literature values of $u(p,T)$ for these liquids (toluene [16], water [17], ethanol [18], and tetrachloromethane [19]). For this purpose we used the following equation

$$1/u = (c_1 + c_2T + c_3T^2) + (c_4 + c_5T + c_6T^2)p^2 + \{(c_7 + c_8T + c_9T^2) + (c_{10} + c_{11}T + c_{12}T^2)p^2\}\Delta\tau. \tag{2}$$

K and K' in equation (1) can thus be empirically determined as a function of T and p. On the basis of the statistical evaluation of the residuals between equation (2) and the literature data of the four calibrating fluids, the overall uncertainty (accuracy) of the SS measurements in the full experimental range of pressure, temperature, and speed of sound is estimated to be of the order of ±0.1 to 0.2. This figure mainly reflects some degree of inconsistency between four distinct data sets since the internal precision is slightly better, ∼±0.05%. This can be judged by the standard deviation of the Pade 3×3 fit (equation (3), see below) to the data points of acetone obtained with this new microcell. In turn, the uncertainty in the measurement of $\Delta\tau$ is $2 \cdot 10^{-10}$ s, which contributes to an uncertainty of ±0.02 to 0.04 $\text{m}\cdot\text{s}^{-1}$ to u, i.e., less than ±0.004%.

Spectroscopic grade acetone, purchased from Merck, with purity better than 99.9% (as checked by gas chromatography) was filtered through 0.2 μm filters and injected into the cell. In the case of the measurements performed with the novel microcell, the liquid is injected under vacuum to insure the complete filling of the cell. The cell itself had previously been placed in a vacuum oven at ~370 K for 24 h to degas the stainless steel and remove traces of water.

This new microcell was tested taking advantage of the parallel measurements we have performed in this work on the speed of sound in acetone using the standard intrusive cell [3] of well-proven reliability. The comparison of the results obtained in the temperature range (288 to 340) K and pressure up to 65 MPa shows that the largest deviations are of the order of 0.2% (see below), which confirms the usefulness of the new cell.

Densities, ρ, in the temperature range (298 to 340) K and pressure range (0.1 to 60) MPa were measured using a previously calibrated Anton Paar DMA 512P vibrating tube densimeter, where temperature is controlled to ±0.01 K and pressure accuracy and precision are better than 0.05%. The overall density precision is typically 0.002%, while its estimated uncertainty (judging by the residuals of the overall fit in comparison with literature data for the calibrating liquids) is 0.02%.

3. Results and discussion

The measured values of the speed of sound and densities of acetone as a function of temperature and pressure are shown in figures 3–5. In the case of the SS, results obtained with this novel cell are compared with those using the standard pulse-eco method (figure 4). Although physical and thermodynamic properties of acetone have been studied for many years, it still appeared that most of the work has been done at room temperature and atmospheric pressure. In particular, using pressure as a variable has been relatively rare. In respect to density, direct measurements over broad ranges of temperature and pressure are practically not available. Actually one needs to extract density from other volumetric measurements and compile data over broader temperature and pressure ranges (French [12], Mahlotra and Woolf [13], Pöhler and Kiran [14]).

Even less data are available for the speed of sound of acetone. Only a few data points are available at atmospheric pressure [20,21] and old data by Eden and Richardson [10] extend the pressure range up to 70 MPa at only three isotherms. The most extensive data on the thermodynamic properties of acetone over broad intervals of temperature (273 to 323) K and pressure (1 to 400) MPa have been given by Malhotra and Woolf [13]. These include calculations of isothermal compressibility (κ_T), isobaric expansivity (α_p) and isobaric heat capacity (c_p). The latter has also been determined directly from calorimetric measurements in the temperature range (273 to 325) K but only for atmospheric pressure (Low and Moelwyn-Hughes [22], Staveley et al. [23], and French [12]; Ibberson et al. [24] reported c_p from the solid region to the liquid up to 300 K). There are no c_p

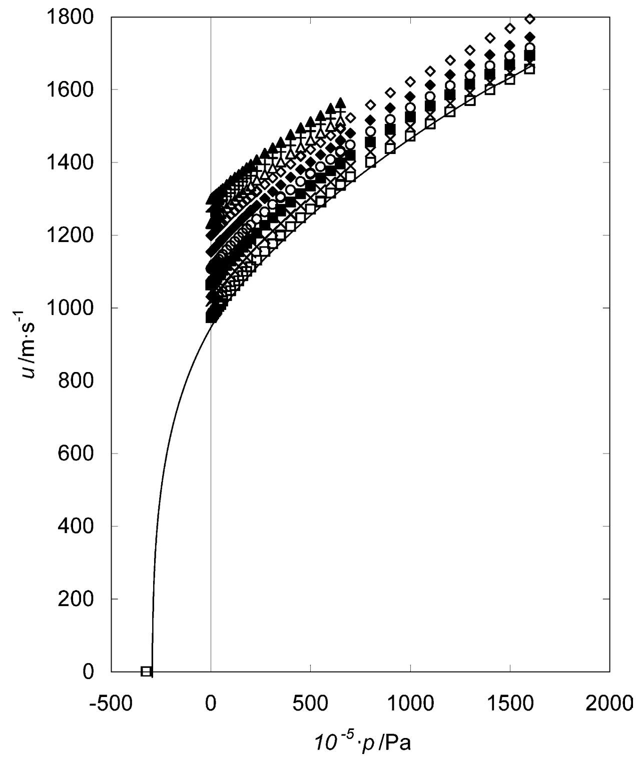

FIGURE 3. Isotherms of the experimental speed of sound, u, in acetone. The line (merely a visual guide) shows, qualitatively, how u has to decrease upon depressurisation in order to meet the null value criterion at the mechanical spinodal locus (at the highest experimental temperature). □, 338.22 K; ×, 328.33 K; ■, 318.22 K; ○, 308.22 K; ◆, 298.23 K; ◇, 288.23 K; △, 280.74 K; +, 273.16 K; ▲, 265.67 K.

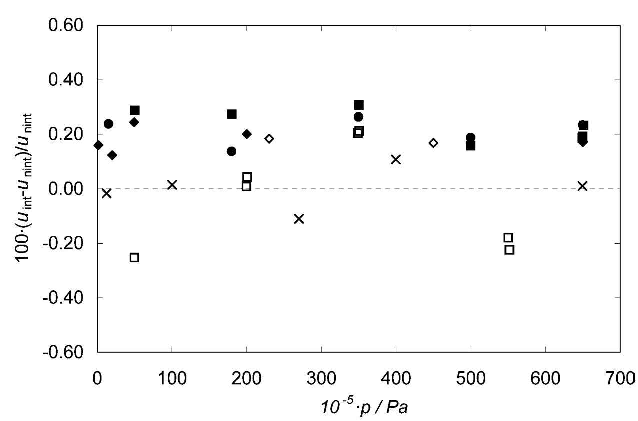

FIGURE 4. Individual experimental data points of u using the non-intrusive (nint) and the standard intrusive (int) methods compared as deviations in percentage. □, 338.22 K; ×, 328.33 K; ■, 318.22 K; ○, 308.22 K; ◆, 298.23 K; ◇, 288.23 K.

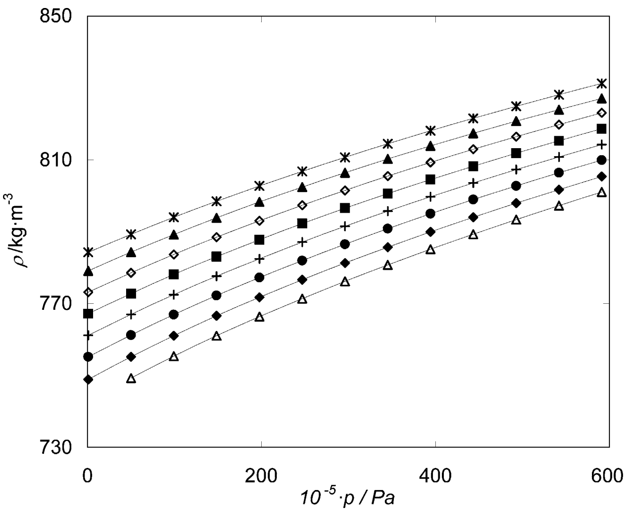

FIGURE 5. Isotherms of the experimental density, ρ, of acetone. △, 333.04 K; ◆, 328.06 K; ●, 322.93 K; +, 317.97 K; ▲, 313.04 K; ◇, 308.08 K; ▲, 303.10 K; ✱, 298.15 K.

data determined from direct calorimetric measurements for higher pressures than the atmospheric one.

The speed of sound raw data (more than 360 points) as a function of both temperature and pressure are reported in table 1. For the sake of economy of size of the table, data are presented for nominal temperatures which, typically, differ from the actual ones by no more than (0.01 or 0.02) K. Note that $(\partial u/\partial T)_p \sim -(4.25 \pm 0.25)\ \mathrm{m \cdot s^{-1} \cdot K^{-1}}$ within the whole T, p range. Original data have been fitted to a Pade 3×3 equation of the form:

$$(u/\mathrm{m \cdot s^{-1}}) = \frac{\sum_{i=0}^{2}\sum_{j=0}^{2} a_{ij}(T/\mathrm{K})^i (p/\mathrm{MPa})^j}{\sum_{k=0}^{2}\sum_{l=0}^{2} b_{kl}(T/\mathrm{K})^k (p/\mathrm{MPa})^l}. \qquad (3)$$

The values of the coefficients were calculated by means of a least-squares analysis of the experimental results (using the algorithm of Marquardt–Levenberg) and are given in table 2. The standard deviation between the experimental and fitted values is found to be 0.08% (0.05% if solely the non-intrusive cell data are considered), which demonstrates the validity of this representation. This fitting equation was screened for thirty isotherms within the experimental temperature range $(265 < T/\mathrm{K} < 340)$, thus in steps of 2.5 K, and for steps of 0.1 MPa within the experimental interval of pressure $(0.1 < p/\mathrm{MPa} < 160)$ for a total of 48,000 data points. No poles for this rational function were found. Also, neither the temperature nor the pressure derivatives of $u(p, T)$ as described by equation (3) present any anomalies. Therefore, equation (3) can be safely used for interpolations.

As mentioned above, the only available experimental data on the pressure dependence of the speed of sound are those published 40 years ago by Eden and Richardson [10]. The comparison of their results with ours, presented for selected isotherms (figure 6), shows bad agreement in the whole pressure range. One should notice that, at lower temperatures, somewhat better agreement is seen for higher pressure while, at higher temperatures, the compared results come closer for lower pressure. A comparison between our density data and theirs reveals similar trends. It is our contention that the analysis of both the speed of sound and density data suggests that their acetone samples certainly contained a non-negligible amount of water and this constitutes the main reason for the observed discrepancies. There exists another single datum point for the speed of sound of acetone reported by Papaionnou et al. [21] at 298.15 K and 0.1 MPa ($u = 1160.6\ \mathrm{m \cdot s^{-1}}$), which agrees reasonably well with our result ($u = 1153.7\ \mathrm{m \cdot s^{-1}}$), but not sufficiently, taking into account our interval of uncertainty. Similarly, we attribute this discrepancy to a higher water content of the literature's sample.

The isothermal plots of the speed of sound versus pressure, shown in figure 3, are not linear showing, instead, obvious curvature, which becomes especially pronounced at higher temperatures. This fact suggests the proximity of the mechanical spinodal line (at which, theoretically, $u = 0$). Below a certain temperature, which is system-to-system dependent, pure substances present a spinodal line for the liquid phase that is located at absolute negative pressures [25]. Negative pressure regimes can be achieved experimentally when the liquid probes metastable conditions of superheated and stretched states [26–28]. The spinodal line can be estimated using the Peng-Robinson equation of state (in the case of acetone, at $T = 338$ K it is found at $p = -32.5$ MPa).

Density raw data as a function of both temperature and pressure are reported in table 3. Our experimental densities agree very well with existing, if scattered, literature data [12–14,21]. If one compares the collected literature data [12–14,21], with the results obtained in this work using a global fitting procedure (see equation (5) and table 4), one concludes that the agreement is better than 0.02%, 0.07%, 0.37%, and 0.06%, respectively. Although the global fitting procedure works very well for the representation of the density values, the differentiation with respect to p and T leads to some irregularities. Therefore, in order to calculate the isothermal compressibility, κ_T, and the isobaric thermal expansivity, α_p, from $\rho\ (p, T)$ data we have decided to follow specific routes. To calculate the isothermal compressibility, κ_T,

$$\kappa_T = \frac{1}{\rho}\left(\frac{\partial \rho}{\partial p}\right)_T, \qquad (4)$$

we used the well defined pressure dependence of density described by the Tait equation for each isotherm:

$$1/\rho = 1/\rho^* + A \ln\{(B + 0.1)/(B + p)\}, \qquad (5)$$

TABLE 1
Experimental speeds of sound u for acetone as a function of temperature T and pressure p

p/MPa	u/(m · s^{-1})
$T = 265.67$ K	
0.102	1298.93
0.504	1301.09
0.750	1302.50
1.003	1303.56
1.255	1304.92
1.501	1306.29
2.007	1308.73
2.506	1311.28
3.005	1313.79
4.004	1318.59
5.004	1323.31
6.005	1328.01
8.002	1338.69
10.001	1349.81
12.001	1358.70
14.003	1366.48
16.05	1375.48
18.001	1384.77
18.001	1384.54
20.003	1394.13
23.001	1407.08
27.004	1425.32
31.003	1439.78
34.997	1455.17
39.999	1476.05
45.002	1494.61
49.999	1511.60
55.001	1528.77
60.002	1548.05
65.000	1564.17
$T = 273.16$ K	
0.102	1264.48
0.504	1266.57
0.750	1267.96
1.003	1269.39
1.255	1270.74
1.501	1272.23
2.007	1275.12
2.506	1277.93
3.005	1281.10
3.005	1281.19
4.004	1287.23
4.004	1286.78
5.004	1291.97
5.004	1292.02
6.005	1296.60
8.002	1306.58
10.001	1316.19
12.001	1325.58
14.003	1335.90
16.005	1346.87
18.001	1355.99
20.003	1363.63
23.001	1376.52
27.004	1394.61
31.003	1412.24
34.997	1428.86
39.999	1446.67
45.002	1467.44
49.999	1485.84
55.001	1504.31
60.002	1520.08
65.000	1538.71
$T = 280.74$ K	
0.075	1233.63
0.075	1232.04
0.504	1234.94
0.750	1236.39
1.003	1237.85
1.255	1239.22
1.501	1240.59
2.007	1243.75
2.506	1247.03
3.005	1249.76
4.004	1255.13
5.004	1259.87
6.005	1264.80
8.002	1275.79
10.001	1286.82
12.001	1296.79
14.003	1306.71
16.005	1316.23
18.001	1325.46
20.003	1335.09
23.001	1350.80
23.001	1350.80
27.004	1366.99
31.003	1384.26
34.997	1401.32
39.999	1423.56
39.999	1423.74
45.002	1441.37
45.002	1441.37
49.999	1461.28
55.001	1480.44
60.002	1498.97
60.002	1498.91
65.000	1514.56
65.000	1514.63
$T = 288.23$ K	
0.109	1199.01
0.504	1201.24
0.750	1202.57
1.003	1204.20
1.255	1205.54
1.501	1206.97
2.007	1209.92
2.506	1212.80
3.005	1215.61
4.004	1221.35
5.004	1227.14
6.005	1232.71
8.002	1244.39
10.001	1255.40
12.001	1265.22
14.003	1275.63
16.005	1286.61
18.001	1296.18
20.003	1305.89
23.001	1319.61
23.004	1322.04*
27.004	1339.05
31.003	1357.37
34.997	1373.83
39.999	1395.08
44.976	1418.48*
45.002	1416.10
49.999	1435.37
55.001	1453.97
60.002	1473.72
64.986	1494.63*
65.000	1492.08
70.010	1522.58*
79.981	1557.72*
89.921	1591.43*
99.957	1621.80*
109.936	1650.70*
119.980	1680.46*
129.872	1708.01*
139.915	1741.66*
149.867	1768.25*
159.874	1794.07*
$T = 298.23$ K	
0.109	1153.69
0.162	1155.53*
0.504	1156.23
0.750	1157.82
1.003	1159.50
1.255	1161.14
1.501	1162.71
2.007	1165.65
2.008	1167.09*
2.506	1168.60
3.005	1171.49
4.004	1177.40
4.938	1185.79*
5.004	1182.90
6.005	1189.60
8.002	1201.45
10.001	1212.80
12.001	1223.83
14.003	1234.83
16.005	1246.18
18.001	1256.46
20.003	1265.92
20.019	1268.46*
23.001	1281.93
27.004	1301.17
31.003	1319.28
34.997	1337.90
39.999	1359.25
45.002	1380.44
49.999	1400.61
55.001	1421.32
60.002	1439.68
65.000	1458.59
65.010	1461.13*
69.929	1479.73*
79.828	1515.66*
89.866	1549.26*
99.836	1580.68*
109.920	1612.39*
119.896	1641.11*
129.797	1668.29*
139.882	1695.55*

TABLE 1 (*continued*)

p/MPa	u/$(m \cdot s^{-1})$
149.849	1721.56*
159.838	1743.99*
$T = 308.22$ K	
0.109	1107.74
0.504	1110.52
0.750	1112.35
1.003	1114.01
1.255	1115.75
1.501	1117.34
1.529	1120.00*
2.007	1120.69
2.506	1123.91
3.005	1127.11
4.004	1133.79
5.004	1140.56
6.005	1146.98
8.002	1159.51
10.001	1171.13
12.001	1182.37
14.003	1194.75
16.005	1205.76
17.995	1218.24*
18.001	1216.57
20.003	1227.49
23.001	1244.05
27.004	1263.44
31.003	1283.97
34.970	1305.89*
34.997	1302.46
39.999	1324.45
45.002	1347.09
49.966	1370.35*
49.999	1367.79
55.001	1388.31
60.002	1408.07
64.978	1431.07*
65.000	1427.73
69.913	1448.08*
80.042	1484.54*
89.948	1517.17*
100.008	1550.07*
109.959	1580.84*
120.002	1610.69*
129.943	1638.63*
139.970	1665.32*
149.805	1691.77*
159.981	1714.52*
$T = 318.22$ K	
0.109	1062.32
0.504	1065.38
0.750	1067.34
1.003	1069.21
1.255	1071.11
1.501	1072.72
2.007	1076.32
2.506	1079.71
3.005	1083.50
4.004	1090.38
5.004	1096.85
5.049	1100.00*
6.005	1103.61
8.002	1116.61
10.001	1129.13
12.001	1142.47
14.003	1154.62
16.005	1166.43
18.001	1177.61
18.039	1180.82*
20.003	1189.14
23.001	1205.63
27.004	1226.77
31.003	1247.41
34.997	1266.28
35.013	1270.18*
39.999	1290.76
45.002	1313.78
49.984	1336.94*
49.999	1334.83
55.001	1356.46
60.002	1376.77
64.915	1398.03*
65.000	1395.43
69.945	1418.97*
79.995	1455.81*
89.950	1490.61*
100.047	1524.64*
109.858	1555.20*
119.927	1585.72*
129.859	1614.28*
139.873	1642.01*
149.838	1668.21*
159.857	1694.12*
$T = 328.22$ K	
0.129	1018.30
0.504	1021.14
0.750	1023.10
1.003	1024.91
1.255	1026.82
1.279	1026.65*
1.501	1028.60
2.007	1032.33
2.506	1036.21
3.005	1040.05
4.004	1047.07
5.004	1053.76
6.005	1060.70
8.002	1074.73
10.001	1088.42
10.021	1088.58*
12.001	1101.14
14.003	1113.97
16.005	1126.49
18.001	1138.92
20.003	1151.08
23.001	1168.10
26.986	1189.14*
27.004	1190.45
31.003	1211.66
34.997	1231.66
39.941	1258.02*
39.999	1256.67
45.002	1280.63
49.999	1303.34
55.001	1324.67
60.002	1345.81
64.927	1365.71*
65.000	1365.57
70.016	1390.37*
79.971	1428.58*
89.947	1463.95*
99.925	1498.01*
109.933	1530.79*
120.024	1561.93*
129.885	1591.12*
139.921	1619.83*
149.939	1647.27*
159.881	1673.62*
$T = 338.22$ K	
0.170	972.80
0.504	976.32
0.750	978.88
1.003	981.05
1.255	982.97
1.501	984.75
2.007	988.42
2.506	992.07
3.005	996.00
4.004	1004.26
5.004	1011.63
5.007	1009.07*
6.005	1019.16
8.002	1033.34
10.001	1047.72
12.001	1061.19
14.003	1074.71
16.005	1088.09
18.001	1100.33
19.962	1112.67*
20.003	1112.58
20.078	1113.05*
23.001	1131.02
27.004	1154.76
31.003	1176.19
34.862	1200.01*
34.997	1197.57
35.061	1200.11*
39.999	1223.29
45.002	1248.14
49.999	1271.19
54.993	1290.41*
55.001	1293.31
55.162	1290.99*
60.002	1315.39
64.959	1338.94*
65.000	1336.38
65.100	1339.48*
70.004	1360.20*
80.065	1399.97*
89.970	1437.71*
99.933	1472.23*
109.905	1505.88*
119.873	1538.58*
129.936	1569.69*
139.985	1599.90*
149.899	1628.37*
159.818	1656.51*

*Measurements performed with the non-intrusive method.

TABLE 2
Coefficients of equation (3) valid within the intervals: $265 < T/\text{K} < 340$ and $0.1 < p/\text{MPa} < 160$

a_{ij}	j		
i	0	1	2
0	$2.55504 \cdot 10^{3}$	$4.28692 \cdot 10^{1}$	-2.20070
1	-8.34018	$-3.19580 \cdot 10^{-1}$	$1.28060 \cdot 10^{-2}$
2	$6.31423 \cdot 10^{-3}$	$7.35340 \cdot 10^{-4}$	$-1.76633 \cdot 10^{-5}$
b_{kl}	l		
k	0	1	2
0	1.00000	$6.32893 \cdot 10^{-2}$	$-1.54202 \cdot 10^{-3}$
1	$-1.20021 \cdot 10^{-3}$	$-5.01416 \cdot 10^{-4}$	$9.37898 \cdot 10^{-6}$
2	$-1.08291 \cdot 10^{-6}$	$1.06248 \cdot 10^{-6}$	$-1.39463 \cdot 10^{-8}$

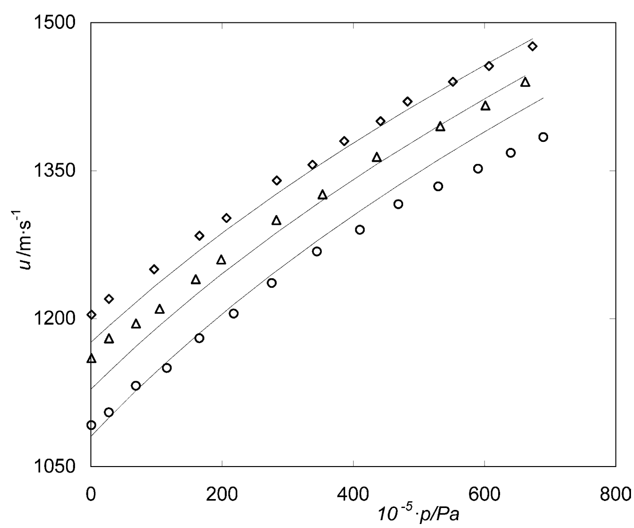

FIGURE 6. Comparison between our interpolated speed of sound data (full lines) for acetone using the Pade 3 × 3 fitting (equation (3)) and the data of Eden and Richardson [10]. ○, 314.15 K; △, 303.65 K; ◇, 293.15 K.

where ρ^* is the density at a given temperature and at a reference pressure of 0.1 MPa. The Tait equation has long proven to constitute a powerful fitting equation even in the low pressure region near orthobaric conditions [29], provided the pressure interval is not extremely broad. Dymond and Malhotra [30] discussed the merits of this equation and its excellent representation of liquid densities up to 150 MPa. Typically, in the current work, the largest residuals for each isotherm of density are of about 0.003%. The coefficients of the fitting equation are given in table 4. The calculated κ_T values for acetone are presented in figure 7 and table 5. Our values of κ_T compare well with those reported by Malhotra and Woolf [13] and Staveley et al. [23]. The deviations are not greater than 2%.

The isobaric thermal expansivity, α_p, defined as:

$$\alpha_p = -\frac{1}{\rho}\left(\frac{\partial \rho}{\partial T}\right)_p \qquad (6)$$

can also be obtained from analytical differentiation of the $\rho(T)$ fitting equation. Unfortunately, there is no analogue of the Tait equation for the temperature dependence. As shown above, many analytical fitting equations can satisfactorily reproduce the experimental densities but at the same time lead to different isobaric thermal expansion coefficients. Because the best choice of method for fitting the $\rho(T)$ data is unclear, several attempts were checked and it was finally decided to use a second order polynomial to individually fit each experimental isobar. The results of α_p are presented in figure 8 and reported in table 6. The agreement between our results and those from literature [13,23] is satisfactory – over the whole temperature and pressure range studied deviations are not greater than 3%.

Densities and speed of sound data can be combined to calculate the isentropic compressibility according to the equation:

$$\kappa_S = \frac{1}{u^2 \rho}. \qquad (7)$$

The calculated isentropic compressibilities are presented in figure 9 and table 7. Estimated uncertainties are less than 1%. Selected points can be compared with the available literature data [21,23] at 0.1 MPa. The agreement is satisfactory, within 2%.

The density and speed of sound data when combined lead to the calculation of isobaric heat capacities through the well known thermodynamic relation:

$$c_p = \frac{T}{\rho}\,\frac{\alpha_p^2}{\kappa_T - \kappa_S}. \qquad (8)$$

In the calculation of isobaric heat capacities, all values for each thermodynamic property expressed in equation (8) were obtained as previously described. For instance, isothermal compressibilities were obtained by pressure differentiation of equation (5), whereas isobaric thermal expansivities were obtained by temperature differentiation of second order polynomials that individually fit each experimental isobar of density (see table 8).

Although the present c_p data agree reasonably well with both reported calculated [13] and experimental [23] (calorimetric) values, the uncertainties associated with the calculated ones can be as high as 7%. In the calculation of c_p, all errors of the previously calculated quantities accumulate, and especially large errors may arise from the difference $(\kappa_T - \kappa_S)$. As for the latter, our results show that the ratio (κ_T/κ_S) in acetone varies, irrespective of temperature, linearly from 1.4 to 1.3 as pressure shifts from (0.1 to 60) MPa. In other words, κ_T is greater than κ_S by 30% to 40%. Taking into account that the accuracy of both κ_T and κ_S is of the order of a

TABLE 3
Experimental densities ρ for acetone at temperatures T and pressures p

p/MPa	ρ/(kg · m^{-3})
T = 298.15 K	
0.100	784.28
5.003	789.28
9.921	794.00
14.838	798.48
19.756	802.74
24.673	806.82
29.591	810.72
34.508	814.46
39.426	818.07
44.343	821.54
49.261	824.89
54.178	828.15
59.096	831.28
T = 303.10 K	
0.100	779.14
5.003	784.32
9.921	789.22
14.838	793.88
19.756	798.30
24.673	802.44
29.591	806.43
34.508	810.24
39.426	813.89
44.343	817.40
49.261	820.77
54.178	823.99
59.096	827.09
T = 308.08 K	
0.100	773.18
5.003	778.55
9.921	783.65
14.838	788.47
19.756	793.02
24.673	797.37
29.591	801.50
34.508	805.47
39.426	809.28
44.343	812.94
49.261	816.44
54.178	819.82
59.096	823.08
T = 313.04 K	
0.100	767.23
5.003	772.79
9.921	778.11
14.838	783.09
19.756	787.80
24.673	792.27
29.591	796.55
34.508	800.60
39.426	804.52
44.343	808.25
49.261	811.85
54.178	815.32
59.096	818.65
T = 317.97 K	
0.100	761.17
5.003	766.99
9.921	772.47
14.838	777.62
19.756	782.47
24.673	787.11
29.591	791.49
34.508	795.70
39.426	799.71
44.343	803.57
49.261	807.28
54.178	810.82
59.096	814.24
T = 322.93 K	
0.100	755.22
5.003	761.27
9.921	766.95
14.838	772.25
19.756	777.28
24.673	781.99
29.591	786.54
34.508	790.84
39.426	795.02
44.343	798.96
49.261	802.75
54.178	806.40
59.096	809.91
T = 328.06 K	
0.100	748.91
5.003	755.20
9.921	761.09
14.838	766.61
19.756	771.75
24.673	776.65
29.591	781.30
34.508	785.72
39.426	789.98
44.343	794.04
49.261	797.97
54.178	801.71
59.096	805.36
T = 333.04 K	
5.003	749.27
9.921	755.39
14.838	761.07
19.756	766.40
24.673	771.41
29.591	776.21
34.508	780.78
39.426	785.17
44.343	789.33
49.261	793.37
54.178	797.25
59.096	801.03

few percent, the calculation of c_p based on equation (8) can still be legitimated, but the difference in the denominator largely contributes to the overall uncertainty of c_p.

Taking into account the relation:

$$c_p/c_v = \kappa_T/\kappa_S, \quad (9)$$

one can calculate the isochoric specific heat capacity according to:

TABLE 4
Coefficients of equation (5) for the density of acetone on each isotherm, valid in the range (0.1 < p/MPa < 60)[a]

T/K	A/$(\mathrm{kg^{-1} \cdot m^3})$	B/MPa	ρ^*/$(\mathrm{kg \cdot m^{-3}})$
298.15	$1.14838 \cdot 10^{-4}$	67.4822	784.332
303.10	$1.15333 \cdot 10^{-4}$	64.1469	778.763
308.08	$1.16241 \cdot 10^{-4}$	61.1206	773.039
313.04	$1.17553 \cdot 10^{-4}$	58.4346	767.217
317.97	$1.19261 \cdot 10^{-4}$	56.0893	761.310
322.93	$1.21386 \cdot 10^{-4}$	54.0563	755.247
328.06	$1.24012 \cdot 10^{-4}$	52.2982	748.849
333.04	$1.26979 \cdot 10^{-4}$	50.9265	742.514

[a] In the case of global fitting procedure one uses $A = 8.33473 \cdot 10^{-4} - 4.87964 \cdot 10^{-6}(T/\mathrm{K}) + 8.28215 \cdot 10^{-9}(T/\mathrm{K})^2$, $B = 869.871 - 4.67571(T/\mathrm{K}) + 6.65600 \cdot 10^{-3}(T/\mathrm{K})^2$, and $\rho^* = 897.862 + 3.51327 \cdot 10^{-1}(T/\mathrm{K}) - 2.45551 \cdot 10^{-3}(T/\mathrm{K})^2$.

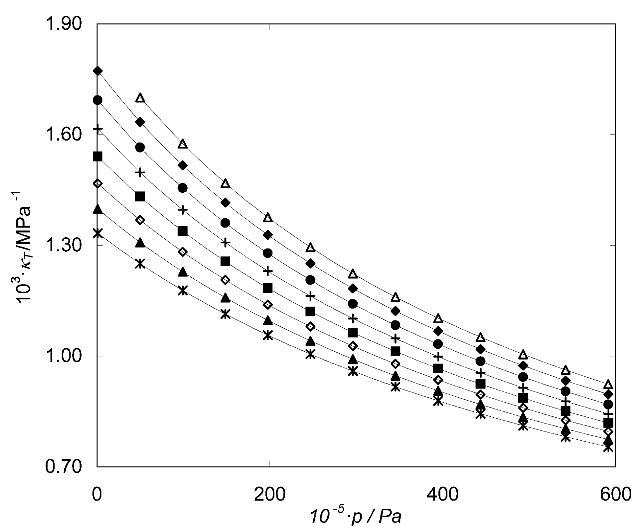

FIGURE 7. Isotherms for the isothermal compressibility of acetone. △, 333.04 K; ◆, 328.06 K; ●, 322.93 K; +, 317.97 K; ■, 313.04 K; ◇, 308.08 K; ▲, 303.10 K; ✱, 298.15 K.

$$c_\mathrm{v} = \frac{T}{\rho} \frac{\alpha_\mathrm{p}^2 \kappa_\mathrm{S}}{\kappa_\mathrm{T}(\kappa_\mathrm{T} - \kappa_\mathrm{S})}. \tag{10}$$

Calculated values compare favourably (within ~5%) with those reported by Staveley et al. [23] for 0.1 MPa. Finally, it is worth to calculate values of the thermal pressure coefficient, γ_v. According to the definition:

$$\gamma_\mathrm{v} = \left(\frac{\partial p}{\partial T}\right)_\mathrm{v} = \frac{\alpha_\mathrm{p}}{\kappa_\mathrm{T}}. \tag{11}$$

Calculated values are in good agreement with data reported by Staveley et al. [23] at 0.1 MPa (within ~3%).

4. Conclusions

The values of calculated thermodynamic properties of acetone are generally in good agreement with the most reliable data found in the literature proving the high quality of the experimentally measured densities and speeds of sound. This, in turn, proves the usefulness of the new microcell for speed of sound measurements in broad temperature and pressure ranges.

TABLE 5
Calculated values of isothermal compressibility κ_T from this work on the experimental isotherms and isobars

p/MPa	T/K							
	298.15	303.10	308.08	313.04	317.97	322.93	328.06	333.04
				$10^3\ \kappa_\mathrm{T}/\mathrm{MPa^{-1}}$				
0.100	1.33_3	1.39_8	1.46_8	1.54_1	1.61_6	1.69_3	1.77_2	
5.003	1.25_0	1.30_8	1.36_8	1.43_2	1.49_8	1.56_5	1.63_4	1.70_0
9.921	1.17_8	1.22_8	1.28_2	1.33_8	1.39_6	1.45_5	1.51_7	1.57_6
14.838	1.11_4	1.15_9	1.20_6	1.25_6	1.30_8	1.36_1	1.41_6	1.46_9
19.756	1.05_7	1.09_7	1.14_0	1.18_4	1.23_1	1.27_8	1.32_8	1.37_6
24.673	1.00_5	1.04_2	1.08_0	1.12_1	1.16_3	1.20_6	1.25_1	1.29_5
29.591	0.95_9	0.99_2	1.02_7	1.06_4	1.10_2	1.14_1	1.18_3	1.22_4
34.508	0.91_7	0.94_7	0.97_9	1.01_3	1.04_8	1.08_4	1.12_2	1.16_0
39.426	0.87_9	0.90_6	0.93_5	0.96_6	0.99_9	1.03_2	1.06_8	1.10_3
44.343	0.84_4	0.86_9	0.89_6	0.92_4	0.95_4	0.98_6	1.01_9	1.05_2
49.261	0.81_1	0.83_5	0.86_0	0.88_6	0.91_4	0.94_3	0.97_4	1.00_5
54.178	0.78_2	0.80_3	0.82_6	0.85_1	0.87_7	0.90_4	0.93_4	0.96_3
59.096	0.75_4	0.77_4	0.79_6	0.81_9	0.84_3	0.86_9	0.89_6	0.92_4

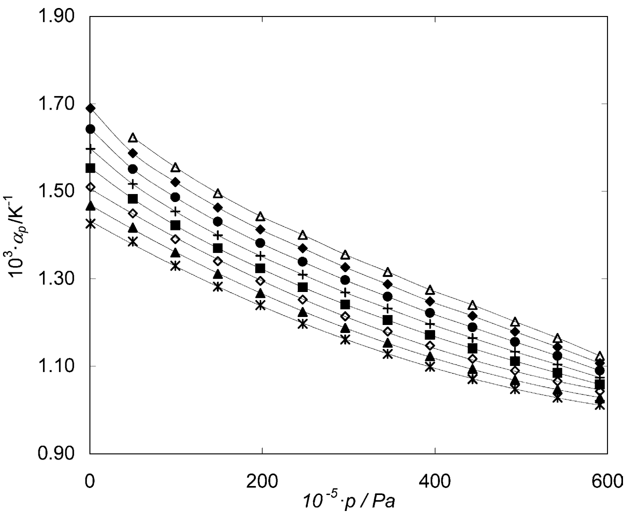

FIGURE 8. Isotherms for the isobaric expansivity of acetone. △, 333.04 K; ◆, 328.06 K; ●, 322.93 K; +, 317.97 K; ■, 313.04 K; ◇, 308.08 K; ▲, 303.10 K; ✱, 298.15 K.

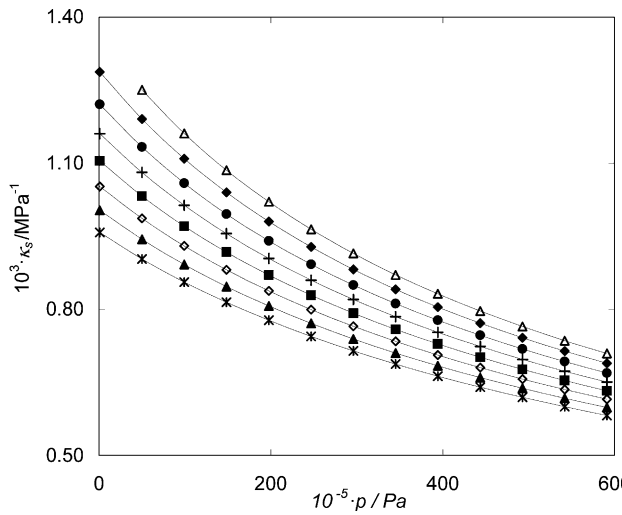

FIGURE 9. Isotherms for the isentropic compressibility of acetone. △, 333.04 K; ◆, 328.06 K; ●, 322.93 K; +, 317.97 K; ■, 313.04 K; ◇, 308.08 K; ▲, 303.10 K; ✱, 298.15 K.

TABLE 6
Calculated values of isobaric thermal expansivity α_p from this work on the experimental isotherms and isobars

p/MPa	T/K							
	298.15	303.10	308.08	313.04	317.97	322.93	328.06	333.04
	$10^3\ \alpha_p$/K^{-1}							
0.100	1.42_6	1.46_7	1.51_0	1.55_3	1.59_7	1.64_2	1.68_9	
5.003	1.38_5	1.41_7	1.44_9	1.48_2	1.51_6	1.55_1	1.58_7	1.62_3
9.921	1.32_9	1.36_0	1.39_1	1.42_2	1.45_4	1.48_6	1.52_1	1.55_5
14.838	1.28_2	1.31_1	1.34_0	1.36_9	1.40_0	1.43_0	1.46_3	1.49_5
19.756	1.24_0	1.26_7	1.29_5	1.32_3	1.35_2	1.38_1	1.41_2	1.44_3
24.673	1.19_7	1.22_4	1.25_2	1.28_1	1.30_9	1.33_9	1.37_0	1.40_0
29.591	1.16_1	1.18_7	1.21_4	1.24_1	1.26_9	1.29_7	1.32_6	1.35_5
34.508	1.12_8	1.15_3	1.17_9	1.20_6	1.23_2	1.25_9	1.28_7	1.31_6
39.426	1.09_9	1.12_3	1.14_7	1.17_1	1.19_6	1.22_2	1.24_8	1.27_5
44.343	1.07_1	1.09_4	1.11_7	1.14_1	1.16_5	1.18_9	1.21_5	1.24_0
49.261	1.04_7	1.06_8	1.09_0	1.11_1	1.13_3	1.15_5	1.17_9	1.20_2
54.178	1.02_8	1.04_7	1.06_5	1.08_5	1.10_4	1.12_3	1.14_4	1.16_4
59.096	1.01_2	1.02_7	1.04_3	1.05_8	1.07_4	1.09_0	1.10_7	1.12_4

TABLE 7
Calculated values of isentropic compressibility κ_s from this work on the experimental isotherms and isobars

p/MPa	T/K							
	298.15	303.10	308.08	313.04	317.97	322.93	328.06	333.04
	$10^3\ \kappa_s$/MPa^{-1}							
0.100	0.95_8	1.00_3	1.05_2	1.10_5	1.16_0	1.22_1	1.28_7	
5.003	0.90_3	0.94_4	0.98_7	1.03_3	1.08_1	1.13_3	1.19_1	1.25_0
9.921	0.85_6	0.89_2	0.93_0	0.97_1	1.01_3	1.05_9	1.10_9	1.16_1
14.838	0.81_4	0.84_7	0.88_1	0.91_7	0.95_5	0.99_6	1.04_0	1.08_5
19.756	0.77_8	0.80_7	0.83_8	0.87_0	0.90_5	0.94_1	0.98_0	1.02_1
24.673	0.74_4	0.77_1	0.79_9	0.82_9	0.86_0	0.89_3	0.92_8	0.96_4
29.591	0.71_5	0.73_9	0.76_5	0.79_2	0.82_0	0.85_0	0.88_2	0.91_5
34.508	0.68_8	0.71_0	0.73_4	0.75_9	0.78_5	0.81_2	0.84_1	0.87_1
39.426	0.66_3	0.68_4	0.70_6	0.72_9	0.75_3	0.77_8	0.80_4	0.83_2
44.343	0.64_0	0.66_0	0.68_1	0.70_2	0.72_4	0.74_7	0.77_1	0.79_7
49.261	0.62_0	0.63_8	0.65_7	0.67_7	0.69_7	0.71_9	0.74_2	0.76_5
54.178	0.60_0	0.61_8	0.63_5	0.65_4	0.67_3	0.69_3	0.71_4	0.73_6
59.096	0.58_2	0.59_9	0.61_6	0.63_3	0.65_1	0.66_9	0.68_9	0.70_9

TABLE 8
Calculated values of isobaric specific heat capacity c_p from this work on the experimental isotherms and isobars

p/MPa	T/K							
	298.15	303.10	308.08	313.04	317.97	322.93	328.06	333.04
				$c_p/(\mathrm{kJ \cdot kg^{-1} \cdot K^{-1}})$				
0.100	2.04_4	2.09_7	2.15_1	2.21_2	2.28_3	2.36_7	2.49_3	
5.003	2.04_8	2.10_3	2.15_9	2.21_9	2.28_8	2.36_8	2.48_9	2.59_7
9.921	2.05_2	2.10_9	2.16_6	2.22_6	2.29_4	2.36_9	2.48_4	2.58_9
14.838	2.05_6	2.11_5	2.17_3	2.23_3	2.29_9	2.37_0	2.48_0	2.58_1
19.756	2.06_0	2.12_1	2.18_1	2.24_0	2.30_5	2.37_2	2.47_6	2.57_2
24.673	2.06_3	2.12_7	2.18_8	2.24_8	2.31_0	2.37_3	2.47_2	2.56_4
29.591	2.06_7	2.13_3	2.19_5	2.25_5	2.31_6	2.37_4	2.46_8	2.55_6
34.508	2.07_1	2.14_0	2.20_3	2.26_2	2.32_1	2.37_5	2.46_4	2.54_8
39.426	2.07_5	2.14_6	2.21_0	2.26_9	2.32_7	2.37_6	2.45_9	2.54_0
44.343	2.07_9	2.15_2	2.21_7	2.27_7	2.33_2	2.37_7	2.45_5	2.53_2
49.261	2.08_2	2.15_8	2.22_5	2.28_4	2.33_8	2.37_8	2.45_1	2.52_4
54.178	2.08_6	2.16_4	2.23_2	2.29_1	2.34_3	2.37_9	2.44_7	2.51_6
59.096	2.08_9	2.16_9	2.23_8	2.29_7	2.34_8	2.38_0	2.44_3	2.50_9

Acknowledgements

This work was financially supported by *Fundação para a Ciência e Tecnologia*, Portugal, under contract POCTI/EQU/34955. R.G.A. and J.M.S.S.E. are grateful to *Fundação para a Ciência e Tecnologia* for doctoral fellowships.

References

[1] J.P.M. Trusler, Physical Acoustics and Metrology of Fluids, Adam Hilger, Bristol, 1991.
[2] G. Douhéret, M.I. Davis, J.C.R. Reis, M.J. Blandamer, Chem. Phys. Chem. 2 (2001) 148–161.
[3] P.F. Pires, H.J.R. Guedes, J. Chem. Thermodyn. 31 (1999) 55–69.
[4] S.J. Ball, J.P.M. Trusler, Int. J. Thermophys. 22 (2001) 427–443.
[5] R.C. Asher, Ultrasonic Sensors, Institute of Physics Publishing, Bristol, 1997.
[6] H.J. McSkimin, in: W.P. Mason (Ed.), Physical Acoustics – Principles and Methods, vol. 1, Part A, Academic Press, New York, 1964 (Chapter 4).
[7] J.L. Daridon, A. Lagrabette, B. Lagourette, J. Chem. Thermodyn. 30 (1998) 607–623.
[8] J.P. Petitet, R. Tufeu, Int. J. Thermophys. 4 (1983) 35–50.
[9] V. Kozhevnikov, D. Arnold, E. Grodzinskii, S. Naurzakov, Fluid Phase Equilib. 125 (1996) 149–157.
[10] H.F. Eden, E.G. Richardson, Acustica 10 (1960) 309–315.
[11] J. Timmermanns, Physico-Chemical Constants of Binary Systems, Interscience, New York, 1950, p. 355.
[12] H.T. French, J. Chem. Thermodyn. 21 (1989) 801–809.
[13] R. Malhotra, L.A. Woolf, J. Chem. Thermodyn. 23 (1991) 867–876.
[14] H. Pöhler, E. Kiran, J. Chem. Eng. Data 42 (1997) 379–383.
[15] Z.S. Kooner, W.A. Van Hook, J. Phys. Chem. 92 (1988) 6414–6426.
[16] M.J.P. Muringer, N.J. Trappeniers, S.N. Biswas, Phys. Chem. Liq. 14 (1985) 273–296.
[17] R. Vedam, G. Holton, J. Acoust. Soc. Am. 43 (1968) 108–116.
[18] T.F. Sun, C.A.T. Seldam, P.J. Kortbeek, N.J. Trappeniers, S.J. Biswas, Phys. Chem. Liq. 18 (1988) 107–116.
[19] A. Lainez, J.F. Miller, J.A. Zollweg, W.B. Streett, J. Chem. Thermodyn. 19 (1987) 1251–1260.
[20] Landolt-Börnstein, Neue Serie, BdII/5, Springer-Verlag, Heidelberg, 1966, p.19.
[21] D. Papaionnou, D. Ziakas, C. Panayiotou, J. Chem. Eng. Data 36 (1991) 35–39.
[22] I.R. Low, E.A. Moelwyn-Hughes, Proc. R. Soc. London A 267 (1962) 384.
[23] L.A.K. Staveley, W.I. Tupman, K.R. Hart, Trans. Faraday Soc. 51 (1955) 323–343.
[24] R.M. Ibberson, W.I.F. David, O. Yamamuro, T. Matsuo, H. Suga, J. Phys. Chem. 99 (1995) 14167–14173.
[25] A. Imre, K. Martinás, L.P.N. Rebelo, J. Non-Equilibrium Thermodyn. 23 (1998) 351–375.
[26] H.I.M. Veiga, L.P.N. Rebelo, M. Nunes da Ponte, J. Szydlowski, Int. J. Thermophys. 22 (2001) 1159–1174.
[27] Z.P. Visak, L.P.N. Rebelo, J. Szydlowski, J. Chem. Educ. 79 (2002) 869–873.
[28] L.P.N. Rebelo, Z.P. Visak, J. Szydlowski, H.I.M. Veiga, R. Gomes de Azevedo, P.F. Pires, M. Nunes da Ponte, in: A.R. Imre, H.J. Maris, P.R. Williams (Eds.), Liquids Under Negative Pressure, NATO Science Series, Kluwer Academic Publishers, Dordrecht, 2002, pp. 95–108.
[29] J.C.G. Calado, H.J.R. Guedes, M. Nunesda Ponte, L.P.N. Rebelo, W.B. Streett, J. Phys. Chem. 90 (1986) 1892–1896.
[30] J.H. Dymond, R. Malhotra, Int. J. Thermophys. 9 (1988) 941–951.

JCT 03/092